NANO · MICRO small

www.small-journal.com

Influence of Chain Architecture on Nanopore Accessibility in Polyelectrolyte Block-Co-Oligomer Functionalized Mesopores

*Robert Brilmayer, Christian Hess, and Annette Andrieu-Brunsen**

Functionalized ordered mesoporous silica materials are commonly investigated for applications such as drug release, sensing, and separation processes. Although, various homopolymer functionalized responsive mesopores are reported, little focus has been put on copolymers in mesopores. Mesoporous silica films are functionalized with responsive and orthogonally charged block-co-oligomers. Responsive 2-dimethylamino)ethyl methacrylate)-block-2-(methacryloyloxy)ethyl phosphate (DMAEMA-*b*-MEP) block-co-oligomers are introduced into mesoporous films using controlled photoiniferter initiated polymerization. This approach allows a very flexible charge composition design. The obtained block-co-oligomer functionalized mesopores show a complex gating behavior indicating a strong interplay between the different blocks emphasizing the strong influence of charge distribution inside mesopores on ionic pore accessibility. For example, in contrast to mesopores functionalized with zwitterionic polymers, DMAEMA-*b*-MEP block-co-oligomer functionalized mesopores, containing two oppositely charged blocks, do not show bipolar ion exclusion, demonstrating the influence of the chain architecture on mesopore accessibility. Furthermore, ligand binding–based selective gating is strongly influenced by this chain architecture as demonstrated by an expansion of pore accessibility states for block-co-oligomer functionalized mesopores as compared to the individual polyelectrolyte functionalization for calcium induced gating.

Inspired by nature and its excellent control over ion transport and ion selectivity, e.g., exemplified by potassium ion channels, as well as inspired by the increasing demand of improved sensor technology in the context of future water management concepts, transport control in technological nanopores becomes increasingly relevant.[1] A wide range of synthetic nanopores has been reported, varying from ion track etched single and multipores in polymer foils, porous polymers as well as inorganic materials such as porous metal oxides or silica based materials.[2] Out of those materials mesoporous silica has been used in various applications due to its high specific surface area, stability, tunable pore characteristics, and adjustable surface chemistry.[3]

The combination of synthetic nanopores with responsive polymers has led to the formation of "smart" nanomaterials as a fascinating research field, achieving increasing interest over the last decade.[4] Responsive hybrid materials can be found in several applications such as separation processes, drug delivery or as chemical sensor.[5] In this context responsive polymers have been used to prepare gates and membranes with adjustable pore accessibility.[6] Polymer functionalization bares the advantage to control pore filling and with this multiplying charges by adjusting chain length and chain density.[7] Various polymerization techniques such as atom transfer radical polymerization (ATRP), reversible addition-fragmentation chain transfer (RAFT), and surface initiated photoiniferter polymerization (SI-PIP) have been studied to graft responsive polymers into nanoscale pores and to vary polymer amount in mesopores.[7a,b,8] In response to stimulation by light, ion concentration, temperature or pH, the surface and pore wall grafted polymers can change their charge, aggregation, and expansion.[4b,c,9] Thereby, pH responsive polymers have been the most extensively studied.[2b,4c,10] This is mainly due to the fact that pH is one of the most important biochemical factors in life processes and can be easily controlled experimentally through acid/base regulation. A wide range of pH responsive polymers that carry a single charge per monomer such as poly(vinylpyridine) (PVP), poly(2-(Dimethylamino)ethyl methacrylate) (PDMAEMA), poly(acrylic acid) (PAA) are reported. In addition multicharged monomers such as (2-(methacryloyloxy) ethyl phosphate) (MEP) or zwitterionic monomers such as carboxybetaine methyl acrylate (CBMA) have been polymerized in nanoporous materials.[2b,4d,6c,d,7a,10a] Additionally, their gating properties and applications have been well investigated.[4e,9,11] Very recent developments going beyond gating focus on asymmetric material structure design being exemplified for example

R. Brilmayer, Prof. A. Andrieu-Brunsen
Ernst-Berl-Institut für Technische und Makromolekulare Chemie
Technische Universität Darmstadt
Alarich-Weiss-Str. 12, 64287 Darmstadt, Germany
E-mail: andrieu-brunsen@smartmem.tu-darmstadt.de

Prof. C. Hess
Eduard-Zintl-Institut für Anorganische und Physikalische Chemie
Technische Universität Darmstadt
Alarich-Weiss-Str. 8, 64287 Darmstadt, Germany

The ORCID identification number(s) for the author(s) of this article can be found under https://doi.org/10.1002/smll.201902710.

DOI: 10.1002/smll.201902710

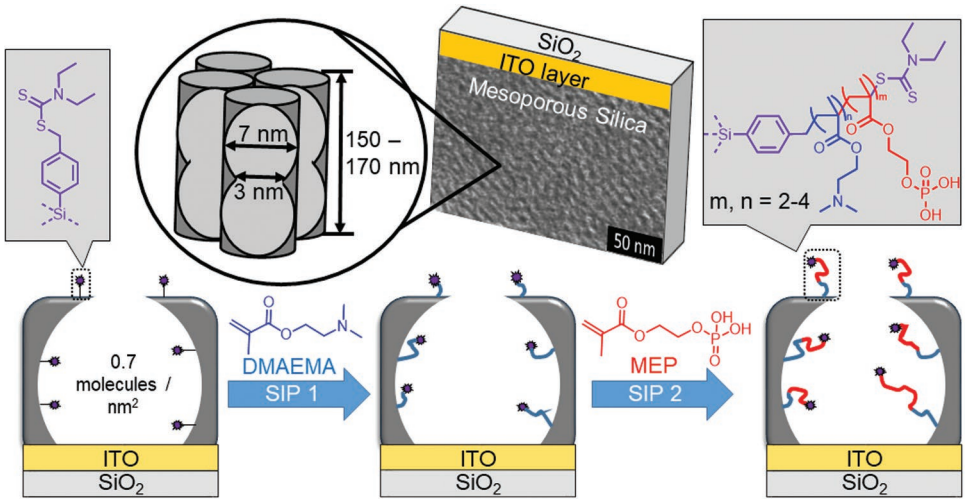

Figure 1. a) Scheme representing block-co-oligomer functionalization of mesoporous silica thin film which are investigated regarding their ionic permselectivity. The mesoporous silica film, displayed in the form of a TEM image, is directly supported on the ITO-coated glass substrate. b) The photoiniferter SBDC is grafted on the outer surface as well as inside the mesopores of the mesoporous silica film. Block-co-oligomer synthesis is performed in two consecutive steps: The first block is synthesized by surface initiated polymerization (SIP) 1 using DMAEMA as monomer. Subsequently, the second block oligomer formation is performed by SIP using MEP as monomer. Chain length of each block (m, n) is determined to be 2–4 repetition units based on X-ray photoelectron spectroscopy and TGA.

by so called Janus membranes enabling side selective or direction dependent oil–water separation or being investigated in the context of ionic energy conversion and the complex interplay of wetting and charge on ionic permselectivity.[5b,12]

Although controlled polymerizations are applied, to our knowledge, responsive polymer functionalized nanoscale pores are limited to homopolymers. On the other hand, it has recently been highlighted by a theoretical work from Szleifer and coworkers that the use of di-block copolymers and statistical block-co-polymers with precise charge composition could be of great use for designing advanced functions and to reach the full potential of smart nanomaterials.[13] Experimentally designing such precisely functionalized nanopores with respect to pore filling and chain architecture control is a challenge. The preparation of DMAEMA-*b*-PMEP diblock containing silica mesopores has previously been demonstrated by our group through reinitiation of Si-PIP polymerization.[7a] A combination of DMAEMA and MEP is expected to be exceptionally interesting for future applications and ion transport investigations because each homopolymer is already known to be multiresponsive, both carry orthogonal charges. PMEP shows two pKa values and thus each monomer can be negatively charged twice and serves as chelating agent for two valent ions such as Ca^{2+}.[6c] DMAEMA on the other hand is known to be temperature- and pH-responsive being able to carry a positive charge per monomer.[14] Combining both into one chain located in a mesopore is expected to result into a functional mesopore, allowing complex transport design in dependence of pore filling, chain architecture and external conditions. Based on these considerations, we herein address the question of oligomer chain architecture influence on the responsive mesopore ionic permselectivity characteristic and report multistimuli responsive and confinement controlled gating properties of PDMAEMA-*b*-PMEP functionalized mesoporous silica thin films varying both simultaneously: the environmental pH and calcium ion presence for highly PDMAEMA-PMEP block oligomer filled mesopores.

Due to their excellent stability and variable structure we choose sol–gel evaporation assembly (EISA) based mesoporous silica thin films as nanoscale porous material. As determined by ellipsometry (Table S1, Supporting Information) and electron microscopy (**Figure 1**), and in accordance with previously reported as-prepared mesoporous silica thin films, the applied mesoporous films have a thickness of ≈200 nm, elliptical mesopores with pore diameters of 6–7 nm and neck diameters of 3 nm, as well as a porosity of ≈45 vol% resulting in ≈440 $m^2\ g^{-1}$ specific surface area.[7a,b]

For the formation of a multiresponsive hybrid material and to investigate the influence of chain architecture and complex charge situation on nanopore permselectivity the photoiniferter (*N*,*N*-(diethylamino)dithiocarbamoyl-benzyl(trimethoxy)silane (SBDC) is postgrafted to the mesopores as shown in Figure 1. The SBDC grafting density has been determined by TGA (thermogravimetric analysis) measurements (Figure S1, Supporting Information) to be 0.7 molecules nm^{-2}. The subsequent SBDC-based surface-initiated polymerizations of 2-(dimethylamino)ethyl methacrylate (DMAEMA) and MEP are performed as previously reported.[7a] Homogeneous distribution of PMEP and Iniferter was proven using cryo-EM (cryogenic electron microscopy) in combination with EDX (energy dispersive X-ray spectroscopy) mapping (data not shown). Through XPS (X-ray photoelectron spectroscopy) measurements of a PDMAEMA-PMEP block-co-oligomer modified film and TGA measurements of PMEP grafted mesoporous silica films the length of each block is determined to be 2–4 repetition units (Figures S5 and S8, Supporting Information). This block-co-oligomer chain ratio of 1:1 is important because it allows to generate an identical number of positive and negative charges within the oligomer chain while charging the individual blocks especially up to a pH value of 7.5 referring to monomer solution pKa values. At pH values higher than 7.5, based on the solution

pKa value, each MEP monomer is expected to generate two negative charges which should turn the overall pore charge to be negative. This result of comparable DMAEMA and MEP oligomer block length is further supported by CV (cyclic voltammetry) measurements. As shown in **Figure 2**d) the peak current density (j_p) for the anionic probe molecule $[Fe(CN)_6]^{3-/4-}$ at acidic pH and the cationic probe molecule $[Ru(NH_3)_6]^{2+/3+}$ at basic pH, and thus the j_p under electrostatic attraction, are comparable.

To first validate the ionic permselectivity and gating properties of the PDMAEMA-*b*-PMEP block-co-oligomer

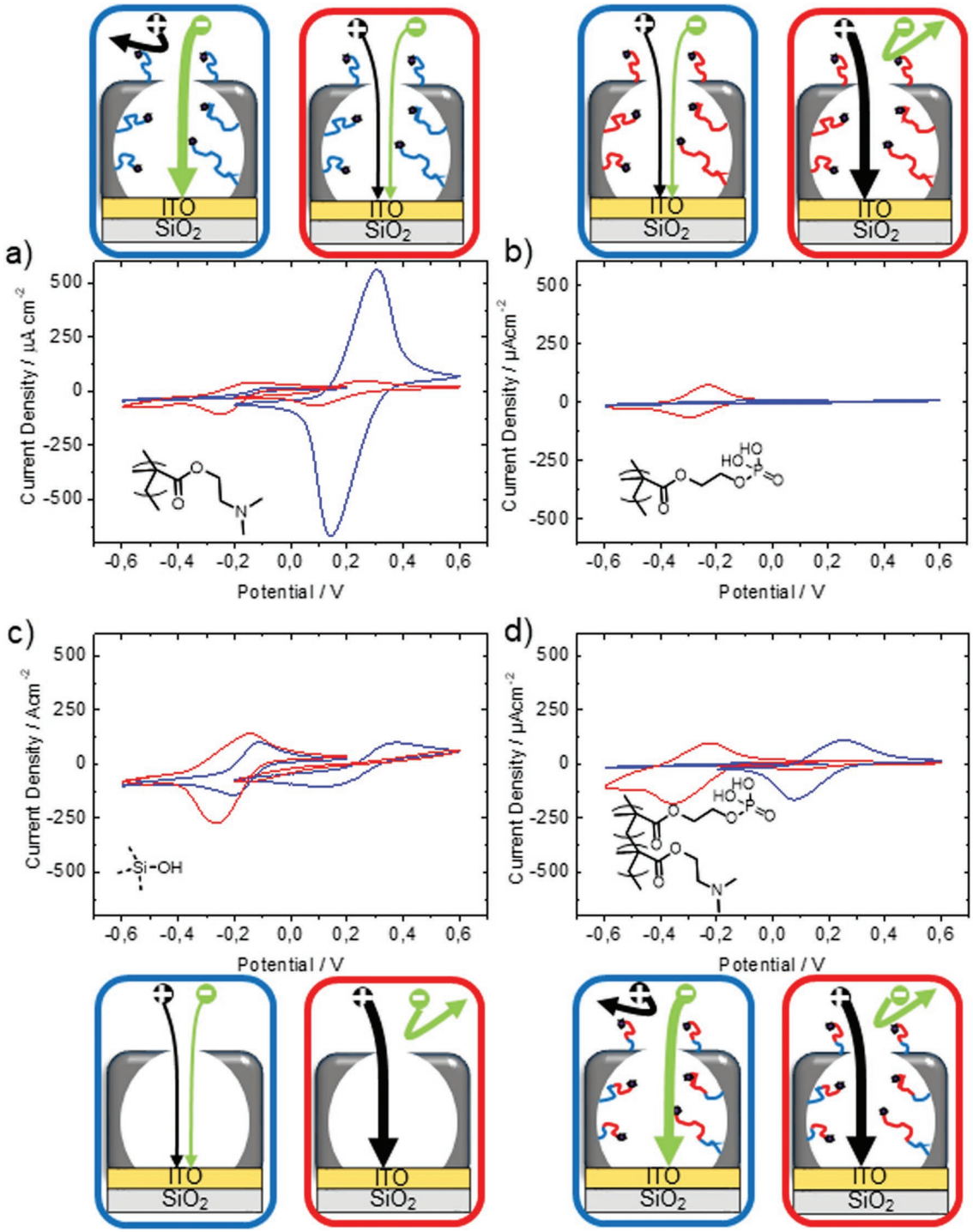

Figure 2. Ionic permselectivity as detected by cyclic voltammetry at an ITO electrode below the mesoporous film for a) PDMAEMA (pore filling 50 vol%), b) PMEP (pore filling 80 vol%), c) unmodified, d) PDMAEMA-*b*-PMEP block-co-oligomer (pore filling 95 vol%) modified mesoporous silica thin films. Cyclic voltamogramms are recorded at a scan rate of 100 mV s^{-1} in a 0.1 M KCl-solution and a 150×10^{-3} M PBS solution in the case of d) at pH 8–9 (red) and pH 2–3 (blue) using $[Fe(CN)_6]^{3-/4-}$ as anionic (–0.2 to 0.6 V) and $[Ru(NH_3)_6]^{2+/3+}$ as cationic probe molecule (–0.6 to 0.2 V).

modified mesoporous silica film, CV measurements are performed (Figure 2). The obtained results are compared with PDMAEMA and PMEP homopolymer-functionalized nanopores (Figure 2a,b) at an acidic (Figure 2 blue) and basic pH value (Figure 2 red). As reference (Figure 2c) the gating behavior of an unmodified mesoporous silica film is shown. The positively charged probe molecule $[Ru(NH_3)_6]^{2+/3+}$ enters the unmodified silica mesopores at acidic (Figure 2c, blue lines) and is slightly preconcentrated at basic (Figure 2c, red lines) pH values. The anionic probe molecule $[Fe(CN)_6]^{3-/4-}$ is excluded at basic pH as expected due to electrostatic repulsion resulting from the deprotonated mesopore wall silanol groups together with the pore diameters within the Debye Screening length. After modification with homo oligomers (Figure 2a for PDMAEMA and Figure 2b for PMEP) mesoporous silica films show inaccessible pores for the probe molecule being identically charged to the pore wall-grafted monomers which is in accordance to corresponding literature studies.[6c,15] For the homo-oligomer modification we choose the same polymerization conditions as for the corresponding blocks of the PDMAEMA-*b*-PMEP block-co-oligomer. Those conditions lead to a pore filling of ≈50 vol% in case of the PDMAEMA modification and ≈80 vol% for the PMEP modification (Table S1, Supporting Information) in initially empty mesopores.[7a] As prepared PDMAEMA-modified mesopores entirely exclude $[Ru(NH_3)_6]^{2+/3+}$ molecules at acidic pH (Figure 2a) and hinder transport (reduced j_p as compared to unfunctionalized mesopores) at basic pH. This effect is even more prominent for PMEP-modified mesopores entirely excluding $[Fe(CN)_6]^{3-/4-}$ molecules (Figure 2b) independently of pH as well as $[Ru(NH_3)_6]^{2+/3+}$ molecules at acidic pH and thus at conditions at which the oligomer is not charged. Reduced j_p values for uncharged pores compared to the mesoporous silica reference can be mainly ascribed to the pore filling with polymer, inducing steric hindrance. A strong influence of the pore filling on the ionic mesopore accessibility can as well be deduced from the j_p obtained under electrostatic attraction between oligomer-functionalized pore and probe molecule: Compared to the mesopore accessibility of $[Ru(NH_3)_6]^{2+/3+}$ into the unmodified mesoporous silica (Figure 2c) film the maximum current density of $[Fe(CN)_6]^{3-/4-}$ in PDMAEMA-modified mesoporous films (Figure 2a) show a significant preconcentration as indicated by the doubled maximum current density. On the other hand, the peak current density of $[Ru(NH_3)_6]^{2+/3+}$ at pH 9 significantly decreases for the PMEP modified mesopores with high pore filling degrees of 80 vol% (Figure 2b) despite the electrostatic attraction between PMEP and $[Ru(NH_3)_6]^{2+/3+}$. These results clearly show the importance of controlling the polymerization and thus the pore filling to tune transport properties either toward higher ion concentration inside the mesopores or toward ion selectivity.

Based on these reference experiments ionic permselectivity of the block-co-oligomer functionalized mesopores with a pore filling degree of 95 vol% has been conducted (Figure 2d).[7a] Thereby our interest was triggered by the behavior of zwitterionically functionalized mesopores showing a bipolar nanopore behavior excluding ions independently of their charge.[10a,16] Designing the PDMAEMA-*b*-PMEP block-co-oligomer functionalization allows to introduce an identical number of opposite charges into one pore and into each polymer/oligomer chain but with a different chain architecture as compared to zwitterionic PCBMA, inducing a different nanoscale order. At an acidic pH the PDMAEMA-*b*-PMEP modified mesoporous silica film (Figure 2d) completely excludes the $[Ru(NH_3)_6]^{2+/3+}$ meanwhile the detected j_p of $[Fe(CN)_6]^{3-/4-}$ ions is comparable to unmodified silica films but does not show a preconcentration as strong as for the PDMAEMA modified mesoporous films. In contrast to this, at a basic pH the PDMAEMA-*b*-PMEP functionalized mesopores show a complete exclusion of $[Fe(CN)_6]^{3-/4-}$ ions while the maximum peak current density for the $[Ru(NH_3)_6]^{2+/3+}$ triples with a current peak density of 180 µA cm^{-2} compared to 53 µA cm^{-2} for the MEP homooligomer modified mesoporous film. From this observation we draw the following two conclusions: The first PDMAEMA block is as visible to ions as the second PMEP block, indicating that the position of the blocks does not significantly determine or hinder ionic permselectivity of such highly filled mesopores and thus the polymer synthesis can be planned purely on synthetic needs at least for the shown degrees of pore filling. Secondly, the maximum current density and thus the probe molecule concentration in the mesopores for block-co-oligomer filled pores are higher than for highly filled PMEP-homo-oligomer functionalized pores indicating that electrostatic attraction dominates and that an interaction between the different repetitions units is probable.

To fully exclude bipolar pore formation, which is not observed for acidic and basic pH (Figure 2d), ionic pore accessibility has been investigated upon gradually changing the solution pH. **Figure 3** shows the maximum peak current densities of the cationic ($[Ru(NH_3)_6]^{2+/3+}$, black spheres) and the anionic ($[Fe(CN)_6]^{3-/4-}$, green spheres) probe molecule at pH values between 2 and 12. From these data it is possible to distinguish three different ion selectivity regimes as illustrated in Figure 3 by the red to blue background color. At acidic pH values below the solution pKa_1 of MEP ($pKa_1 = 4.5$), the pore is purely anion selective (red background color regime in Figure 3b) with a nondetectable peak current density for the cationic probe molecule $[Ru(NH_3)_6]^{2+/3+}$. At these acidic pH values the pore is positively charged due to the PDMAEMA block. Starting at a solution pH of around 4 the maximum peak current density of the anionic probe molecule $[Fe(CN)_6]^{3-/4-}$ decreases by 35% from 242 to 160 µA cm^{-2} and stays constant until a pH of 8. Under the same conditions the maximum peak current density of the cationic probe molecule increases until it reaches the same peak current density as detected for the anionic probe molecule at pH 7.5–8. This second, neutral region between pH 4 and 8 has been identified to be between the pKa of DMAEMA (8.4) and the pKa_1 of MEP ($pKa_1 = 4.5$), resulting in both blocks being charged. This regime, indicated in violet color in Figure 3, is characterized by an increasing number of charged MEP repetition units of the block oligomer while the DMAEMA monomers are expected to stay positively charged. The existence of both charges can be expected since otherwise the detected maximum peak current density would be much smaller as visible in Figure 2a) and b) due to the mesopores being filled with polymer. The 3rd transport regime starts close to the solution pKa of DMAEMA at pH 8. The detected maximum peak current density for the anionic probe molecule in this basic pH range finally drops rapidly from 170 to almost

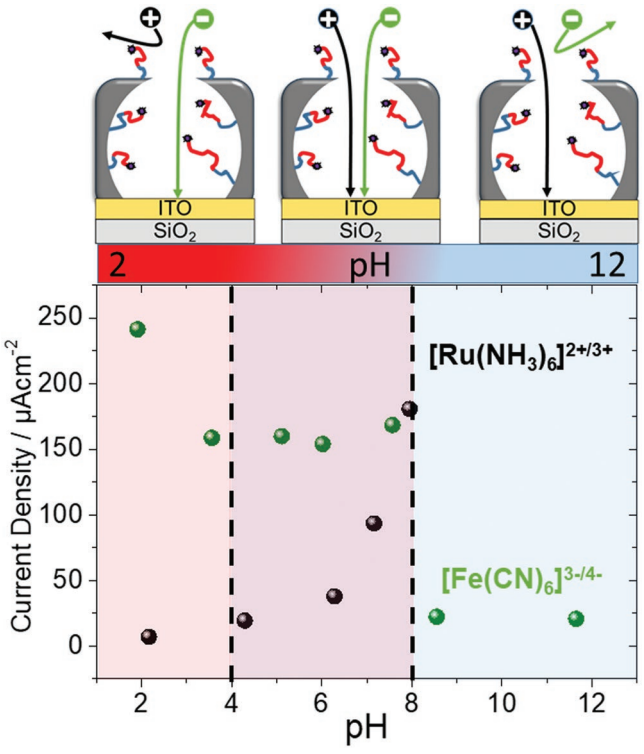

Figure 3. Pore scheme of a PDMAEMA-*b*-PMEP block-co-oligomer modified mesopore and its ionic permselectivity behavior with varying solution pH value. The measured ionic permselectivity can be gradually adjusted from anion selective at acidic pH (red area) over an open state between approximately pH 4–8 to a cation selective nanopore at basic pH (blue area). This observation is based on the pH-dependent current peak densities of $[Fe(CN)_6]^{3-/4-}$ (green spheres) and $[Ru(NH_3)_6]^{2+/3+}$ (black spheres) recorded at an ITO electrode below the mesoporous film at a scan rate of 100 mV s^{-1} in a 150×10^{-3} M PBS solution at solution pH values between 2 and 12.

20 µA cm^{-2} resulting into a cation selective pore (Figure 3 blue coded regime). Interestingly, these PDMAEMA-*b*-PMEP block oligomer with both monomers charged or partially charged obviously behave differently than mesopores functionalized with zwitterionic oligomers which exclude both, anions as well as cations, being described as bipolar pores.[16,17] This bipolar behavior is not observed for the described PDMAEMA-*b*-PMEP block-co-oligomer functionalized mesopores although, positive and negative charges are simultaneously present in each polymer chain within a mesopore, too. Thus, the polymer/oligomer chain architecture, anion and cation confined into each monomer for zwitterionic polymers versus separation of anions and cations into a block like sequence seems to crucially affect the resulting ionic mesopore accessibility. This behavior might be partially due to interactions between the blocks of different oligomer chains, which surely get in contact in such a confined environment as an 8 nm pore. The measurements described were performed at an ionic strength of 150×10^{-3} M which corresponds to a Debye Screening length of ≈0.9 nm. Since the Debye Screening length can play a crucial role on pore accessibility and thus on ion selectivity, additional measurements at an ionic strength of 30×10^{-3} M were performed (Figure S2c,d, Supporting Information). These measurements showed no significant difference with respect to charge selectivity of the modified mesoporous silica films under the applied measurement conditions as well supporting high pore filling degrees. In addition to its double pH responsiveness, PMEP bares the potential to investigate ligand binding and selective gating because it chelates divalent cations such as Ca^{2+}. Both aspects strongly influence transport related applications such as (bio)separation and sensing in which a variety of ions is present and selective interaction is required. In a previous work we demonstrated two-valent ion induced gating of PMEP functionalized mesopores at basic pH resulting in similar ionic pore accessibility characteristics as for acidic pH conditions.[6c] Here, we are systematically addressing significantly higher pore filling degrees (23 vol% vs up to >80 vol%) as well as the chain architecture. By comparing purely PMEP functionalized pores to PDMAEMA-*b*-PMEP block-co-oligomer functionalized mesopores. As a first result the high pore-filling degress of ≈80 vol% for PMEP functionalized mesopores block the pore for $[Fe(CN)_6]^{3-/4-}$ probe molecules as already shown in Figure 2. The presence of calcium ions does not affect this behavior (Figure S2b, Supporting Information). Nevertheless, the pore accessibility for electrostatically attracted $[Ru(NH_3)_6]^{2+/3+}$ probe molecules behaves as expected (**Figure 4**a black vs green). The maximum peak current density significantly decreases upon addition of calcium from initially 60 to 20 µA cm^{-2} due to the blocking of PMEP charges and thus decreasing electrostatic attraction. Additionally the redox peak potential shifts which seems to indicate electrostatic attraction (Figure S2c, Supporting Information). This leads also to a decrease in the pH responsiveness of the system. Upon the addition of Ca^{2+}-ions (2×10^{-3} M) to the solution the cyclic voltammograms do not vary significantly when measured at a solution pH of 2 and 11 (Figure S2a, Supporting Information). In addition, the chelation between the MEP and calcium ions is clearly transport limited and equilibrium is reached after ≈30 min (Figure 4a different colors) as well supporting the influence of high pore filling degrees. Upon addition of Ca^{2+}-ions to PDMAEMA-*b*-PMEP block-co-oligomer functionalized mesopores (Figure 4b) the effect of chain architecture on ionic pore accessibility again becomes very clear. In contrast to purely PMEP functionalized mesopores no effect of calcium ions on ionic pore accessibility (j_p) is observed for PDMAEMA-*b*-PMEP functionalized mesoporous films at basic pH (Figure 4b). Whereas calcium ions strongly affect ionic pore accessibility at pH values between 2 and 7.5 corresponding to the anion selective and neutral pH regime in Figure 3. This strongly indicates an interaction between calcium ions and PMEP still at acidic pH which implicates, in contrast to the expectation based on solution pKa values, that PMEP still is not fully neutralized within this pH range. This is additionally supported by the j_p, indicating a significant preconcentration for $[Fe(CN)_6]^{3-/4-}$ probe molecules in this pH-range (Figure 4b). Comparing the maximum peak current density of PDMAEMA-*b*-PMEP block-co-oligomer functionalized mesopores in the absence of calcium (Figure 4b spheres, Figure 2d) this is much lower as for purely PDMAEMA functionalized pores under identical conditions (acidic pH, Figure 2a red). Upon addition of calcium ions to PDMAEMA-*b*-PMEP block-co-oligomer functionalized mesopores with a pore filling degree of ≈95 vol% (Figure 4b, red star, pH 2) the pore accessibility and thus the measured

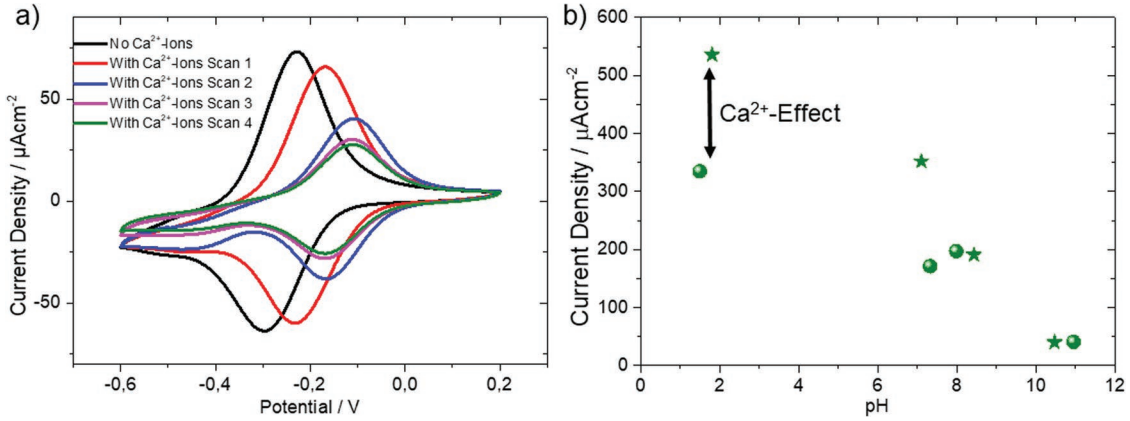

Figure 4. a) Cyclic voltamogramms of a PMEP modified mesoporous silica film before (black line) and after addition of Ca^{2+}-ions into the bulk solution in dependence of time after addition (red 0 min, blue 7 min, pink 14 min, and green 21 min). Measurements are recorded using $[Ru(NH_3)_6]^{2+/3+}$ as probe molecule at a scanrate of 100 mV s^{-1} in a 150×10^{-3} M PBS solution at a solution pH of 11. b) Current peak densities of a PDMAEMA-*b*-PMEP modified mesoporous silica film using $[Fe(CN)_6]^{3-/4-}$ as probe molecule and recorded at a scan rate of 100 mV s^{-1} in a 1× PBS solution (150×10^{-3} M) at pH values between 2 and 12 in the presence (stars) and absence (spheres) of 2×10^{-3} M $CaCl_2$.

maximum peak current density increases by 200 µA cm^{-2} corresponding to a factor of 1.6–2 and reaches values of ≈535 µA cm^{-2} comparable to purely PDMAEMA functionalized mesopores with a pore filling degree of ≈80 vol%. This fully inversed transport behavior of the block-co-oligomer functionalized mesopores compared to homooligomer functionalized mesopores demonstrates the strong influence of the charge composition and chain architecture. This is an essential aspect in approaching nature's pore design and transport control precision and with this implementing and pushing nanopore transport dependent technologies. Our results are a first experimental step toward this direction allowing multifunctionality combined with precise design in pore filling and chain architecture, although still being less precise as theoretical studies implicate with respect to monomer positioning along a polymer chain.[13]

Precise design of nanopore functionalization, and not only the choice of functional polymers, strongly determines their ionic accessibility and transport performance. Pore filling limits transport especially if no electrostatic attraction exists. Nevertheless, this effect can be overcompensated by precise chain architecture and charge composition design. Based on functionalization of mesopores with block-co-oligomer polyelectrolytes, composed of pH-responsive and orthogonally charged blocks, a complex transport behavior differing from the homo-oligomer functionalized mesopores has been implemented. This functionalization has been achieved by reinitiation of controlled iniferter-initiated polymerization. PDMAEMA-*b*-PMEP functionalized mesopores with high pore filling degrees of up to 95 vol% have been gradually tuned from anion to cation selective depending on solution pH. Thereby no bipolar pore behavior, as reported for zwitterionic polymer modified mesopores, is observed in pH-regimes in which both blocks should be orthogonally charged. This demonstrates the importance of oligomer chain architecture design for ionic mesopore permselectivity. Finally, ligand binding and selective gating is strongly influenced by this chain architecture. We demonstrate that the pore opening and closing behavior can be expanded by using block-co-oligomer polyelectrolytes PDMAEMA-*b*-PMEP as compared to the individual polyelectrolytes PDMAEMA and PMEP. All together this functionalization and the observed complex transport control offers a toolbox to fine tune mesopore transport based on pore filling degrees and block-co-oligomer ratios allowing to approach nature's design precision. Especially if the precision of chain design will be further improved, e.g., by using peptide synthesis and precise combinations and placement of chargeable or ligand binding functional units. This fine tuning is expected to advance technologies depending on pore accessibility and transport control such as sensors or (bio)separation and water management.

Experimental Section

Surface-Initiated Polymerization (SIP) of DMAEMA-b-MEP: Following the literature procedure by Tom et al. the block-co-oligomer functionalization was done in two consecutive steps.[7a] As a first step surface-initiated polymerization (SIP) (1), DMAEMA (2.0 mL, 11.8 mmol) were dissolved in dry DMF (16 mL). To this solution, a SBDC functionalized mesoporous silica film deposited on an ITO coated glass substrate was added before the mixture was sealed with a rubber septum and deoxygenated by nitrogen bubbling for 5 min before irradiation using a Bio-Link BLX by Vilber Lourmat (t = 5 min, λ = 365 nm, P = 40 W). The substrates were subsequently extracted through multiple washing steps with DMF and distilled H_2O. For the subsequent second SIP, SIP (2), MEP (0.55 g) was dissolved in distilled H_2O (20 mL). The substrate was added to this solution before the mixture was sealed using a rubber septum and deoxygenated for 15 min before irradiation using a Bio-Link BLX by Vilber Lourmat (t = 15 min, λ = 365 nm, P = 40 W). Finally, the substrates were extracted in distilled water overnight.

Supporting Information

Supporting Information is available from the Wiley Online Library or from the author.

Acknowledgements

The authors acknowledge funding from the Hessen State Ministry of Higher Education, Research and the Arts, Germany, in the frame of the

LOEWE project iNAPO. The authors thank Nicole Herzog for her help with XPS and TEM sample preparation and Karl Kopp for performing XPS measurements. The authors also thank Ulrike Kunz and Prof. Kleebe from the department of Materials Science of the Technische Universität Darmstadt for their support with TEM measurements and Prof. Markus Biesalski for access to interface characterization facilities.

Conflict of Interest

The authors declare no conflict of interest.

Keywords

confinement effects, ionic permselectivity, mesoporous silica, multiresponsive gating, polyelectrolyte block copolymers

Received: May 25, 2019
Revised: August 12, 2019
Published online: August 25, 2019

[1] a) D. M. Mitrano, E. Rimmele, A. Wichser, R. Erni, M. Height, B. Nowack, *ACS Nano* **2014**, *8*, 7208; b) D. A. Doyle, J. M. Cabral, R. A. Pfuetzner, A. Kuo, J. M. Gulbis, S. L. Cohen, B. T. Chait, R. MacKinnon, *Science* **1998**, *280*, 69.

[2] a) A. Walcarius, *Chem. Soc. Rev.* **2013**, *42*, 4098; b) B. Yameen, M. Ali, R. Neumann, W. Ensinger, W. Knoll, O. Azzaroni, *Chem. Commun.* **2010**, *46*, 1908; c) J. Weber, L. Bergstrom, *Langmuir* **2010**, *26*, 10158.

[3] a) G. J. Soler-Illia, O. Azzaroni, *Chem. Soc. Rev.* **2011**, *40*, 1107; b) L. Nicole, C. Boissière, D. Grosso, A. Quach, C. Sanchez, *J. Mater. Chem.* **2005**, *15*, 3598; c) C. J. Brinker, Y. Lu, A. Sellinger, H. Fan, *Adv. Mater.* **1999**, *11*, 579; d) D. R. Dunphy, P. H. Sheth, F. L. Garcia, C. J. Brinker, *Chem. Mater.* **2015**, *27*, 75.

[4] a) H. Zhang, Y. Tian, L. Jiang, *Nano Today* **2016**, *11*, 61; b) F. Xia, L. Jiang, *Adv. Mater.* **2008**, *20*, 2842; c) X. Hou, W. Guo, L. Jiang, *Chem. Soc. Rev.* **2011**, *40*, 2385; d) M. Tagliazucchi, O. Azzaroni, I. Szleifer, *J. Am. Chem. Soc.* **2010**, *132*, 12404; e) M. Ulbricht, *Polymer* **2006**, *47*, 2217.

[5] a) M. H. Sun, S. Z. Huang, L. H. Chen, Y. Li, X. Y. Yang, Z. Y. Yuan, B. L. Su, *Chem. Soc. Rev.* **2016**, *45*, 3479; b) Z. Zhang, X. Sui, P. Li, G. Xie, X. Y. Kong, K. Xiao, L. Gao, L. Wen, L. Jiang, *J. Am. Chem. Soc.* **2017**, *139*, 8905.

[6] a) G. Perez-Mitta, W. A. Marmisolle, A. G. Albesa, M. E. Toimil-Molares, C. Trautmann, O. Azzaroni, *Small* **2017**, *14*, 1702131; b) F. M. Gilles, M. Tagliazucchi, O. Azzaroni, I. Szleifer, *J. Phys. Chem. C* **2016**, *120*, 4789; c) A. Brunsen, C. Diaz, L. I. Pietrasanta, B. Yameen, M. Ceolin, G. J. Soler-Illia, O. Azzaroni, *Langmuir* **2012**, *28*, 3583; d) H. Zhang, X. Hou, L. Zeng, F. Yang, L. Li, D. Yan, Y. Tian, L. Jiang, *J. Am. Chem. Soc.* **2013**, *135*, 16102.

[7] a) J. Tom, R. Brilmayer, J. Schmidt, A. Andrieu-Brunsen, *Polymers* **2017**, *9*, 539; b) L. Silies, H. Didzoleit, C. Hess, B. Stühn, A. Andrieu-Brunsen, *Chem. Mater.* **2015**, *27*, 1971; c) M. Kruk, *Isr. J. Chem.* **2012**, *52*, 246.

[8] a) J. O. Zoppe, N. C. Ataman, P. Mocny, J. Wang, J. Moraes, H. A. Klok, *Chem. Rev.* **2017**, *117*, 1105; b) E. M. Benetti, C. Kang, J. Mandal, M. Divandari, N. D. Spencer, *Macromolecules* **2017**, *50*, 5711; c) H. K. S. B. de Boer, M. P. L. Werts, E. W. van der Vegte, G. Hadziioannou, *Macromolecules* **2000**, *33*, 349; d) J. Jiang, X. Xiao, P. Zhao, H. Tian, *J. Polym. Sci., Part A: Polym. Chem.* **2010**, *48*, 1551; e) J. Elbert, M. Gallei, C. Rüttiger, A. Brunsen, H. Didzoleit, B. Stühn, M. Rehahn, *Organometallics* **2013**, *32*, 5873; f) T. Otsu, A. Kuriyama, *J. Macromol. Sci.,– Chem.* **1984**, *21*, 961; g) K. Matyjaszewski, *Macromolecules* **2012**, *45*, 4015; h) L. Cao, M. Kruk, *Polym. Chem.* **2010**, *1*, 97; i) C. Barner-Kowollik, T. P. Davis, J. P. A. Heuts, M. H. Stenzel, P. Vana, M. Whittaker, *J. Polym. Sci., Part A: Polym. Chem.* **2003**, *41*, 365.

[9] S. P. Adiga, D. W. Brenner, *J. Funct. Biomater.* **2012**, *3*, 239.

[10] a) B. Yameen, M. Ali, R. Neumann, W. Ensinger, W. Knoll, O. Azzaroni, *J. Am. Chem. Soc.* **2009**, *131*, 2070; b) G. Chen, S. Das, *J. Appl. Phys.* **2015**, *117*, 185304.

[11] D. F. Stamatialis, B. J. Papenburg, M. Gironés, S. Saiful, S. N. M. Bettahalli, S. Schmitmeier, M. Wessling, *J. Membr. Sci.* **2008**, *308*, 1.

[12] a) A. Brunsen, J. Cui, M. Ceolin, A. del Campo, G. J. Soler-Illia, O. Azzaroni, *Chem. Commun.* **2012**, *48*, 1422; b) Z. Wang, X. Yang, Z. Cheng, Y. Liu, L. Shao, L. Jiang, *Mater. Horiz.* **2017**, *4*, 701; c) Y. Feng, W. Zhu, W. Guo, L. Jiang, *Adv. Mater.* **2017**, *29*, 1702773; d) H. Cheng, Y. Zhou, Y. Feng, W. Geng, Q. Liu, W. Guo, L. Jiang, *Adv. Mater.* **2017**, *29*, 1700177; e) G. Xie, L. Wen, L. Jiang, *Nano Res.* **2016**, *9*, 59.

[13] K. Huang, I. Szleifer, *J. Am. Chem. Soc.* **2017**, *139*, 6422.

[14] a) C. S. Hang, J. M. Shik, Y. S. Hong, L. H. Bang, *J. Polym. Sci., Part B: Polym. Phys.* **1997**, *35*, 595; b) H. Lee, S. H. Son, R. Sharma, Y. Y. Won, *J. Phys. Chem. B* **2011**, *115*, 844.

[15] N. Herzog, J. Kind, C. Hess, A. Andrieu-Brunsen, *Chem. Commun.* **2015**, *51*, 11697.

[16] L. Silies, A. Andrieu-Brunsen, *Langmuir* **2017**, *34*, 807.

[17] A. Calvo, B. Yameen, F. J. Williams, G. J. A. A. Soler-Illia, O. Azzaroni, *J. Am. Chem. Soc.* **2009**, *131*, 10866.